

BEPPOSAX OBSERVATION OF 4U 1626–67: DISCOVERY OF AN ABSORPTION CYCLOTRON RESONANCE FEATURE

M. ORLANDINI, D. DAL FIUME, AND F. FRONTERA¹

Istituto Tecnologie e Studio Radiazioni Extraterrestri, CNR, via Gobetti 101, 40129 Bologna, Italy; orlandini@tesre.bo.cnr.it

S. DEL SORDO, S. PIRAINO, A. SANTANGELO, AND A. SEGRETO

Istituto Fisica Cosmica e Applicazioni all'Informatica, CNR, via La Malfa 153, 90146 Palermo, Italy

AND

T. OOSTERBROEK AND A. N. PARMAR

Astrophysics Division, ESA, Space Science Department, ESTEC, Keplerlaan 1, 2200 AG Noordwijk, Netherlands

Received 1997 October 30; accepted 1998 April 20; published 1998 June 8

ABSTRACT

We report on an observation of the low-mass X-ray binary 4U 1626–67 performed during the *BeppoSAX* science verification phase. An absorption feature at ~ 37 keV, which is attributable to electron cyclotron resonance, has been discovered in its pulse-averaged spectrum. The inferred neutron star magnetic field strength is $3.2(1+z) \times 10^{12}$ G, where z is the gravitational redshift. The feature is deep and narrow and is resolved in both the broadband fit and in the ratio of observed counts to those seen from the Crab pulsar. The cyclotron resonance energy is in good agreement with the empirical relation between cyclotron energy and high-energy cutoff, while its width is in agreement with the expected Doppler broadening of thermal electrons at the cyclotron resonance frequency. The broadband 0.1–200 keV spectrum is well fit by a two-component model: a 0.27 ± 0.02 keV blackbody and a power law with a photon index of 0.89 ± 0.02 . This is the first broadband observation made after the change from spin-up to spin-down that occurred in mid-1990: it confirms the harder spectrum with respect to those observed in the 2–10 keV range.

Subject headings: binaries: close — pulsars: individual (4U 1626–67) — stars: neutron — X-rays: stars

1. INTRODUCTION

Following the first detection in Her X-1 (Trümper et al. 1978), line features in the 10–110 keV energy range were detected in some X-ray pulsars (Makishima & Mihara 1992; Grove et al. 1995). These features are interpreted as being due to electron cyclotron transitions in the $\geq 10^{12}$ G magnetic field of the neutron star (Makishima & Mihara 1992). Because the energy of the fundamental cyclotron harmonic E_{cyc} is related to the neutron star magnetic field strength B_{12} in units of 10^{12} G by the relation $E_{\text{cyc}} = 11.6B_{12}(1+z)^{-1}$ keV, where z is the gravitational redshift, the observation of cyclotron resonance features (CRFs) in pulsar spectra gives a direct measurement of the magnetic field of the neutron star. From a theoretical point of view, CRFs are expected to be visible as absorption features. This was shown, e.g., by Nagel (1981) for any reasonable optical depth. The feature is not strictly due to absorption but rather to scattering of photons in the wings of the line. Until now, CRFs have been observed mainly in the spectra of young high-mass binary systems, with the notable exception of Her X-1 (Trümper et al. 1978).

The 7.7 s X-ray pulsar 4U 1626–67 is one of the few pulsators among low-mass X-ray binaries. Its timing history is characterized by a sudden change in its spin state that occurred in 1990 June (Chakrabarty et al. 1997). Before this date the source was steadily spinning up, while from the transition to the present time 4U 1626–67 is spinning down. Besides coherent pulsation, 4U 1626–67 also shows quasi-periodic oscillations (QPOs) both in X-rays (Shinoda et al. 1990) and in the optical (Chakrabarty 1998), with a centroid frequency of ~ 40 mHz.

The pulse-phase averaged spectrum of 4U 1626–67 has been

described in terms of a two-component model: an absorbed blackbody with a temperature $kT \sim 0.6$ keV and a power law (Kii et al. 1986). The spectrum also exhibits a high-energy cutoff at ~ 20 keV, which is interpreted as being due to a possible CRF at that energy (Pravdo et al. 1979), and an emission Ne line complex at ~ 1 keV (Angelini et al. 1995). While the spin transition did not affect the high-energy part of the spectrum, within the accuracy of previous measurements, it did affect the 2–10 keV part (Vaughan & Kitamoto 1997): the power-law photon index changed from ~ 1.6 (Pravdo et al. 1979) to ≤ 0.7 (Angelini et al. 1995), with a correspondingly significantly lower 2–10 keV flux that shows an overall fading by a factor 4 from the *HEAO 1/A2* measurement (Chakrabarty et al. 1997).

2. OBSERVATIONS

The *BeppoSAX* satellite is a program of the Italian Space Agency, with participation of the Netherlands Agency for Aerospace Programs, which is devoted to X-ray astronomical observations in the broad 0.1–300 keV energy band. The payload includes four narrow field instruments (NFIs) and two wide field cameras. The NFIs consist of concentrators/spectrometers (C/S) with three units (MECS) operating in the 1–10 keV energy band (Boella et al. 1997) and one unit (LECS) operating in 0.1–10 keV (Parmar et al. 1997), a high-pressure gas scintillation proportional counter (HPGSPC) operating in the 3–120 keV energy band (Manzo et al. 1997), and a phoswich detection system (PDS) with four scintillation detection units operating in the 15–300 keV energy band (Frontera et al. 1997).

During the science verification phase, a series of well-known X-ray sources were observed in order to check the capabilities and performance of the instruments on board *BeppoSAX*. 4U 1626–67 is one of these sources, and it was observed by

¹ Also at the Physics Department, Ferrara University, via Paradiso 12, 44100 Ferrara, Italy.

TABLE 1
BEST-FIT SPECTRAL PARAMETERS^a

PARAMETER	VALUE		
	No Line	Gaussian	Lorentzian
N_H (10^{21} cm ⁻²)	1.1 ± 0.2	1.2 ± 0.2	1.1 ± 0.2
kT (keV)	0.28 ± 0.01	0.29 ± 0.01	0.30 ± 0.01
r_{bb} ($\times d_{kpc}$ km)	1.5 ^{+0.3} _{-0.2}	1.5 ± 0.2	1.4 ± 0.2
α	0.87 ± 0.01	0.86 ± 0.01	0.83 ± 0.01
E_c (keV)	21.1 ± 0.4	19.6 ± 0.5	29 ± 2
E_f (keV)	7.8 ± 0.3	10.6 ± 0.7	9 ⁺² ₋₁
I_{pow}^b	1.06 ± 0.02	1.05 ± 0.02	1.01 ± 0.02
E_{Ne} (keV)	1.05 ^c	1.05 ^c	1.05 ^c
σ_{Ne} (keV)	0.04 ^c	0.04 ^c	0.04 ^a
EW_{Ne} (keV)	48 ^c	48 ^c	48 ^c
E_{CRF} (keV)	...	37 ± 1	33 ± 1
σ_{CRF} (keV)	...	3 ± 1	12 ⁺³ ₋₂
EW_{CRF} (keV)	...	15 ± 3	...
τ_{CRF}	1.6 ± 0.3
χ_r^2	1.369 (706)	1.232 (703)	1.146 (703)

^a Uncertainties at the 90% confidence level for a single parameter.

^b Flux is in units of 10^{-2} photons cm⁻² s⁻¹ at 1 keV.

^c The Ne line complex parameters are taken from Owens et al. 1997.

BeppoSAX on 1996 August 6 from 14:41 to 21:50 UTC and from 1996 August 9 00:10 to August 11 00:00. Data were telemetred in direct modes, which provides complete information on time, energy, and, if available, position for each photon. The net exposure times for the four NFIs were 31, 97, 43, and 52 ks for LECS, each of the MECS units, HPGSPC, and PDS, respectively. These differences are due to the LECS being operated only in satellite nighttime, rocking of collimators (for HPGSPC and PDS), and different filtering criteria during passages in the South Atlantic Geomagnetic Anomaly and before and after Earth occultations. Furthermore, HPGSPC data from the August 6 observation were not included because of telemetry problems. The spurious spikes ($\Delta t \lesssim 2$ s) that affect the PDS data were also filtered. These spikes occur at a frequency of a few per orbit, can reach several hundreds counts per second, and are likely due to the local environmental particle background. Their spectrum is generally soft, showing a strong cutoff at ~ 40 keV (Guainazzi & Matteuzzi 1997). Their presence can severely affect both a spectral and timing analysis, especially for moderately faint sources in the PDS bandpass such as 4U 1626–67.

The data analysis of all the NFIs but the LECS was carried out in the XAS V2.0 framework (Chiappetti & Dal Fiume 1997). For the LECS data, the SAXLEDAS V1.4.0 was used (Lammers 1997). We used the 1997 September revisions of the response matrices for all NFIs but LECS, for which we used the matrix generated by LEMAT V3.5.3.

3. SPECTRAL ANALYSIS

The analysis of the LECS data has been already presented (Owens, Oosterbroek, & Parmar 1997) and will not be discussed here; we will include their results on the Ne line complex. For the imaging instruments, the standard extraction radius of $8'$ was used to derive the source events. The rocking collimated instruments (HPGSPC and PDS) net counts were obtained with the standard background subtraction procedure, which was described in detail in Manzo et al. (1997) and Frontera et al. (1997). The systematic error in PDS background subtraction is consistent with zero for observations longer than

100 ks and is negligible for sources whose flux is higher than 1 mCrab, such as 4U 1626–67 (Guainazzi & Matteuzzi 1997).

3.1. The X-Ray Continuum

The spectra of each *BeppoSAX* NFI were first fitted separately in order to derive the best model able to describe the broadband spectrum. We find that a model including low-energy absorption, a blackbody, a power law, and a high-energy cutoff adequately describes all of the NFI spectra but the PDS, yielding χ_r^2 s of 1.13 (81 degrees of freedom [dof]) for LECS, 1.11 (540 dof) for MECS, 1.29 (144 dof) for HPGSPC, and 1.89 (56 dof) for PDS. Most of the contribution to the high χ_r^2 for PDS is due to deviations at ~ 35 keV. We used this model to describe the broadband 0.1–200 keV spectrum. We included in the fit a variable normalization for each of the NFIs (we treated separately each MECS unit) in order to take into account the known calibration uncertainties between the instruments. As a high-energy cutoff, we used the standard X-ray pulsar model $\exp[(E_c - E)/E_f]$, where E_c and E_f are the cutoff and folding energy, respectively (White, Swank, & Holt 1983). The smoother Fermi-Dirac cutoff (Tanaka 1986) did not adequately describe the high-energy tail. After the inclusion of the Ne line complex at 1 keV, we obtained a best fit with a reduced χ_r^2 of 1.369 for 706 dof. The fit results are summarized in Table 1. The normalizations among NFIs (MECS2 as reference) are 1.04 for LECS, 1.05 for HPGSPC, and 0.72 for PDS.

Our data do not show the presence of an iron *K*-shell line in 6.4–6.9 keV: the 3σ upper limit on its equivalent width is 21 eV, which is slightly more stringent than the 33 eV value obtained by *ASCA* (Angelini et al. 1995). The total 0.1–200 keV X-ray luminosity is 7.7×10^{34} ergs s⁻¹ d_{kpc}^2 . The fluxes in the bands 2–10, 10–60, and 10–200 keV are 1.7, 4.4, and 4.5×10^{-10} ergs cm⁻² s⁻¹, respectively.

3.2. Cyclotron Resonance

From the analysis of the residuals, we were led to add an extra component to our spectral model. Both a Lorentzian (Mihara 1995) or a Gaussian in absorption (Soong et al. 1990) at ~ 35 keV, interpreted as a CRF, improved the fit, yielding χ_r^2 s of 1.146 and 1.232, respectively, for 703 dof. An *F*-test shows that the improvement is significant at 99.99%. Adding this component improved the fit to the 15–200 keV PDS spectrum, yielding a χ_r^2 of 1.256 (53 dof; probability of chance improvement equal to 2.4×10^{-5}). The Gaussian line FWHM of 7 ± 2 keV is consistent with the PDS energy resolution at the CRF energy, $\sim 17.5\%$ (Frontera et al. 1997). Figure 1 shows the best-fitting spectral model with the residual CRF Gaussian line profile obtained by setting the line normalization to zero. The residuals for each NFI are also shown.

The two CRF models are equivalent: the probability of chance improvement from the Lorentzian to the Gaussian model is 34%. The different E_{CRF} found with the two models is an effect due to the modeling: the Lorentzian model approximates the falloff of the spectrum by increasing the cutoff energy and shifting the cyclotron energy to values lower than those obtained by an absorption Gaussian (compare, in Table 1, the best-fit continuum parameters with the CRF line included with those obtained from the continuum without the line). This is a known effect, already having been observed for the CRF in Her X-1 (Dal Fiume et al. 1998) and Vela X-1 (Orlandini et al. 1998).

Following the suggestion by Pravdo et al. (1979) of a pos-

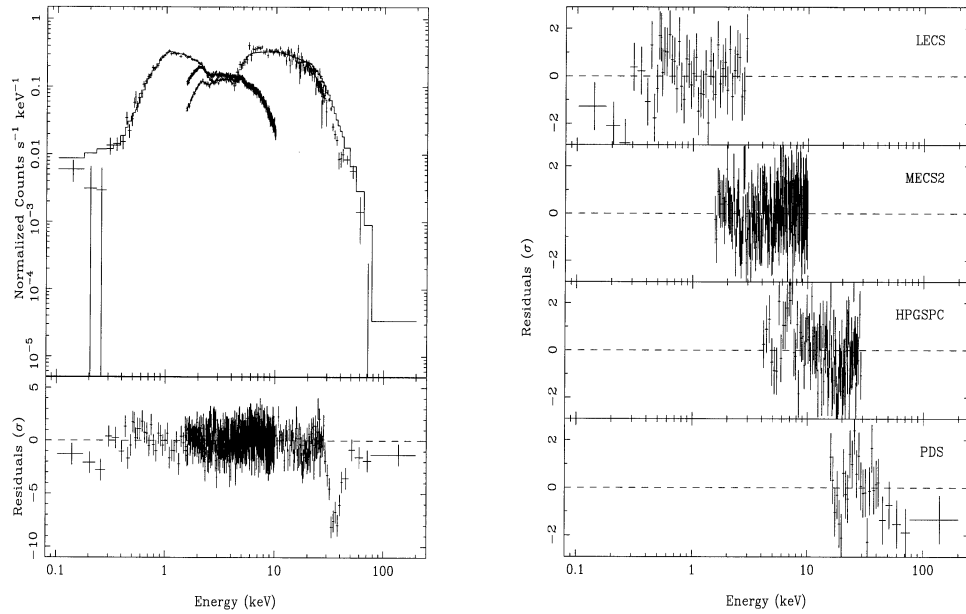


FIG. 1.—Broadband 0.1–200 keV spectrum of 4U 1626–67 observed by the *BeppoSAX* NFIs. *Left*: Count rate spectrum (*plus signs*) and best-fitting continuum model (*histogram*) with the Ne complex and absorption Gaussian components (parameters from Table 1). The Gaussian normalization has been set to zero, and the residuals from the model are shown. *Right*: Detailed NFI residuals from the broadband best-fit model (for clarity, only one MECS unit is shown).

sible CRF at ~ 19 keV, we tried to include in our broadband model a fundamental CRF at this energy (and to therefore consider the ~ 35 keV CRF as the second harmonic). This attempt was unsuccessful, both with and without the high-energy cutoff component.

In order to better characterize the 4U 1626–67 CRF, we

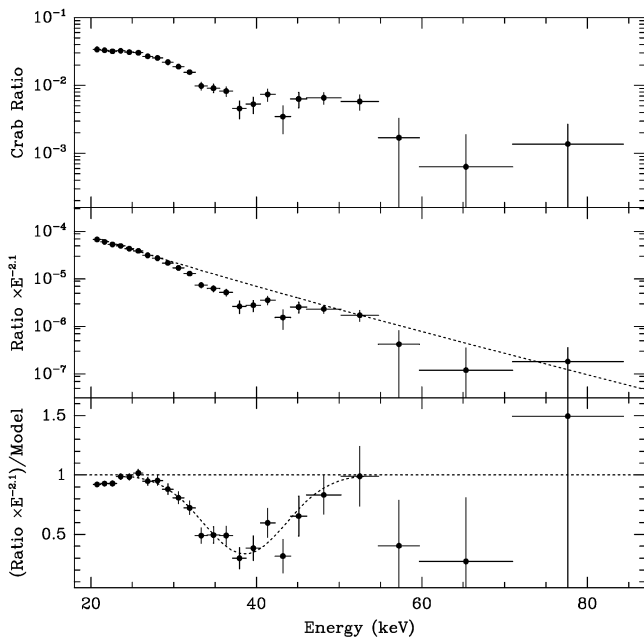


FIG. 2.—*Top*: Ratio between the PDS 4U 1626–67 and Crab count rate spectra. Note the change of slope at ~ 35 keV. *Middle*: 4U 1626–67/Crab ratio multiplied by $E^{-2.1}$, the functional form of the Crab spectrum. Deviations from the continuum (*dotted line*) occur for $E \geq 30$ keV. *Bottom*: Ratio between the 4U 1626–67/Crab ratio times $E^{-2.1}$ and the model of the 4U 1626–67 continuum as derived from the broadband fit. A Gaussian fit to the CRF (*dotted line*) is also shown.

examined the ratio between the PDS and Crab pulsar count rate spectra. This ratio has the advantage of minimizing the effects due to the detector response and the uncertainties in the calibrations. As we can see from the upper panel in Figure 2, there is an evident change of slope at ~ 35 keV. The same ratios performed on the Her X-1 (Dal Fiume et al. 1998) and the Vela X-1 (Orlandini et al. 1998) spectra show a change of slope at ~ 40 and ~ 57 keV—their well-known cyclotron energies.

To enhance the effect due to the CRF, we multiplied the 4U 1626–67/Crab ratio by the functional form of the Crab pulsar spectrum, i.e., a simple power law with an index equal to 2.1. In this way we emphasize deviations of the 4U 1626–67 spectrum from its continuum without making any assumption on its form. The result is shown in the second panel of Figure 2, where it is evident that deviations occur only at $E \geq 30$ keV.

Finally, in the lower panel we show the ratio between the previous function and the 4U 1626–67 continuum model, with α , E_c , and E_f taken from Table 1. In this way we enlarge all of the effects due to line features, although we introduce a model dependence. The absorption feature at ~ 38 keV is evident. This feature can be fit between 25 and 50 keV with both a Gaussian (shown in the figure) and a Lorentzian. The results are shown in Table 2 and are in agreement with those obtained from the broadband spectral fit shown in Table 1. The difference in the σ_{CRF} values is the effect due to the intrinsic energy resolution of the PDS instrument. The inferred magnetic field

TABLE 2

FIT RESULTS ON THE 4U 1626–67
CYCLOTRON RESONANCE FEATURE^a

CRF Parameter	Gaussian	Lorentzian
E_{CRF} (keV)	38.6 ± 0.9	38.1 ± 0.9
σ_{CRF} (keV)	5.0 ± 0.7	8 ± 1
χ^2_{ν} (dof)	1.048 (13)	2.725 (13)

^a Uncertainties are given at the 90% confidence level.

strength at the neutron star surface is therefore $(3.2 \pm 0.1) \times 10^{12} (1+z)$ G, where z is the gravitational redshift.

4. DISCUSSION

This is the first 4U 1626–67 broadband spectrum obtained after the spin transition. From our flux measurement, we can see that the overall *bolometric* flux of the source decreased by a factor of 4.1 since the *HEAO 1/A2* measurements. We find a power-law index slightly higher than those found in narrow-band spectra (Angelini et al. 1995; Owens et al. 1997). This is an effect due to the broadband fit, in which we simultaneously take into account both the low-energy power law and the high-energy cutoff.

Our 4U 1626–67 CRF measurement, together with its cutoff energy, fits the empirical relation found in X-ray binary pulsars between these parameters: the higher the cyclotron resonance energy, the higher the cutoff—and therefore, the harder the spectrum (Makishima et al. 1990; Frontera & Dal Fiume 1989). Our CRF measurement is also in agreement with the expected electron Doppler broadening. Indeed, at the cyclotron resonance frequency ω_c , electrons at rest absorb photons of energy $\hbar\omega_c$. For moving, thermal electrons, the Doppler broadening $\Delta\omega_D$ is predicted to be (Mészáros 1992)

$$\Delta\omega_D = \omega_c \left(\frac{2kT_e}{m_e c^2} \right)^{1/2} |\cos \theta|, \quad (1)$$

where kT_e is the electron temperature, and $m_e c^2$ is the electron rest mass. The angle θ measures the direction of the magnetic field with respect to the line of sight. Outside the range $\omega_c \pm \Delta\omega_D$, the cyclotron absorption coefficient decays exponentially, and other radiative processes become important. From equation (1) and the CRF parameters given in Table 1, we obtain a lower limit to the electron temperature of ~ 5 keV, which is in reasonable agreement with the calculations of self-emitting atmospheres of Harding et al. (1984), according to which the temperature for a column or slab with optical depth ~ 50 g cm^{-2} is $(4-8) \times 10^7$ K, corresponding to $kT_e \sim 3.5-7$ keV.

Finally, we want to mention that if we assume that the quasi-periodic oscillation frequency is due to the beating between the pulse frequency and the Keplerian motion at the magnetospheric radius, then the 4U 1626–67 magnetic field strength is related to its luminosity by the relation $B_{12} \sim 5.5 \sqrt{L_{37}}$ (Shinoda et al. 1990), where L_{37} is the X-ray luminosity in units of 10^{37} ergs s^{-1} . Assuming a source distance $5 \lesssim d_{\text{kpc}} \lesssim 13$ (Chakrabarty 1998), this corresponds to $2.4 \lesssim B_{12} \lesssim 6.3$, which is in good agreement with our measurement.

The authors wish to thank the *BeppoSAX* Scientific Data Center staff, the Nuova-Telespazio OCC personnel, the *BeppoSAX* Mission Scientist L. Piro, and the *BeppoSAX* Mission Director R. C. Butler. This research has been funded in part by the Italian Space Agency. We thank the anonymous referee for useful suggestions.

REFERENCES

- Angelini, L., et al. 1995, *ApJ*, 449, L41
 Boella, G., et al. 1997, *A&AS*, 122, 327
 Chakrabarty, D. 1998, *ApJ*, 492, 342
 Chakrabarty, D., et al. 1997, *ApJ*, 474, 414
 Chiappetti, L., & Dal Fiume, D. 1997, in *Proc. Fifth International Workshop on Data Analysis in Astronomy*, ed. L. Scarsi & M. C. Maccarone (Singapore: World Scientific), 101
 Dal Fiume, D., et al. 1998, *A&A*, 329, L41
 Frontera, F., Costa, E., Dal Fiume, D., Feroci, M., Nicastro, L., Orlandini, M., Palazzi, E., & Zavattini, G. 1997, *A&AS*, 122, 357
 Frontera, F., & Dal Fiume, D. 1989, in *Proc. 23rd ESLAB Symposium on Two Topics in X-ray Astronomy. I. X-Ray Binaries*. (SP-296; Noordwijk: ESA), 57
 Grove, J. E., et al. 1995, *ApJ*, 438, L25
 Guainazzi, M., & Matteuzzi, A. 1997, Technical Report TR-11, *BeppoSAX Scientific Data Center*
 Harding, A. K., Mészáros, P., Kirk, J. K., & Galloway, D. J. 1984, *ApJ*, 278, 369
 Kii, T., Hayakawa, S., Nagase, F., Ikegami, T., & Kawai, N. 1986, *PASJ*, 38, 751
 Lammers, U. 1997, *The SAX/LECS Data Analysis System User Manual*, SAX/LEDA/0010
 Makishima, K., & Mihara, T. 1992, in *Frontiers of X-Ray Astronomy*, ed. Y. Tanaka & K. Koyama (Tokyo: Universal Academy Press), 23
 Makishima, K., et al. 1990, *ApJ*, 365, L59
 Manzo, G., Giarrusso, S., Santangelo, A., Ciralli, F., Fazio, G., Piraino, S., & Segreto, A. 1997, *A&AS*, 122, 341
 Mészáros, P. 1992, *High-Energy Radiation from Magnetized Neutron Stars* (Chicago: Univ. Chicago Press)
 Mihara, T. 1995, Ph.D. thesis, Univ. Tokyo
 Nagel, W. 1981, *ApJ*, 251, 278
 Orlandini, M., et al. 1998, *A&A*, 332, 121
 Owens, A., Oosterbroek, T., & Parmar, A. N. 1997, *A&A*, 324, L9
 Parmar, A. N., et al. 1997, *A&AS*, 122, 309
 Pravdo, S. H., et al. 1979, *ApJ*, 231, 912
 Shinoda, K., Kii, T., Mitsuda, K., Nagase, F., Tanaka, Y., Makishima, K., & Shibazaki, N. 1990, *PASJ*, 42, L27
 Soong, Y., Gruber, D. E., Peterson, L. E., & Rothschild, R. E. 1990, *ApJ*, 348, 641
 Tanaka, Y. 1986, in *Radiation Hydrodynamics in Stars and Compact Objects*, ed. D. Mihalas & K. H. Winkler (Berlin: Springer), 198
 Trümper, J., Pietsch, W., Reppin, C., Voges, W., Staubert, R., & Kendziorra, E. 1978, *ApJ*, 219, L105
 Vaughan, B. A., & Kitamoto, S. 1998, *ApJ*, submitted
 White, N. E., Swank, J. H., & Holt, S. S. 1983, *ApJ*, 270, 711